Geochimica et Cosmochimica Acta, Vol. 69, No. 6, pp. 1405–1411, 2005

0016-7037/05 $30.00 + .00

doi:10.1016/j.gca.2004.08.030

The influence of edge sites on the development of surface charge on goethite nanoparticles: A molecular dynamics investigation

JAMES R. RUSTAD[1,*] and ANDREW R. FELMY[2]

[1]Department of Geology, University of California, Davis, California 95616 USA
[2]Pacific Northwest National Laboratory, Richland, Washington 99352 USA

(*Received April* 20, 2004; *accepted in revised form August* 23, 2004)

Abstract—Large-scale molecular simulation of proton accumulations were carried out on (i) (110) and (021) slabs immersed in aqueous solution and (ii) a series of model goethite nanoparticles of dimension 2 to 8 nm with systematically varying acicularity and (110)/(021) surface areas. In the slab systems, the (021) surface exhibits 15% more proton charge per unit area than the (110) surface. In the particulate systems, the acicular particles having the highest (110)/(021) ratio accumulate the most charge, opposite to the trend expected from the slab simulations, indicating that, at length scales on the order of 10 nm, the slab results are not a good indicator of the overall charging behavior of the particles. The primary reason for the discrepancy between the particulate systems and slab systems is the preferential accumulation of protons at acute (110)-(110) intersections. Charge accumulates preferentially in this region because excess proton charge at an asperity is more effectively solvated than at a flat interface. *Copyright © 2005 Elsevier Ltd*

1. INTRODUCTION

The extent of protonation of oxide surfaces has a fundamental influence on virtually every aspect of their chemical behavior in aqueous systems, governing dissolution/precipitation, sorption, and redox reactions, and controlling the mobility and aggregation state of colloidal-sized particles (Morel and Hering, 1993; Sposito, 2004). Much attention has been focused on relating proton surface charging to oxide surface structure. The current intellectual framework for progress in understanding mineral surfaces reactivity has been built on a series of well-defined systems of increasing complexity (Brown et al., 1999). For the oxides, a systematic path starts by investigating surfaces in vacuum environments and attempting to relate UHV surface structures to bulk structures (e.g., in iron oxide systems: Wang et al., 1998; Rustad et al., 1999; Chambers et al., 2000). These surfaces are then exposed to small amounts of water to ascertain the extent of dissociation and binding energies (Stirniman et al., 1996; Henderson et al., 1998; Kendelewicz et al., 2000). Solvated surfaces are then studied with surface sensitive X-ray scattering techniques (Fenter et al., 2000; Trainor et al., 2002; Zhang et al., 2004). At each level, information is fed upwards. Computational methods have been useful in amalgamating experimental results making up this framework (e.g., for oxides: McCarthy et al., 1996; Wasserman et al., 1997; Hass et al., 1998; Parker et al., 1999; Lodziana et al., 2003; Shapovalov et al., 2003; Zhang et al., 2004).

Surfaces may have different reactivities due to variations in the coordination of oxide surface functional groups comprising the surface (Hiemstra et al., 1989; Hiemstra and VanRiemsdijk, 1996; Rustad et al., 1996), anisotropic surface dielectric properties (Sverjensky and Sahai, 1996; Koretsky et al., 1998), or from the influence of interfacial solvent structure. Once the structures and reactivities of individual surfaces are worked out, it seems natural to assume that a given particle behaves as a composite of its participating surfaces (Felmy and Rustad, 1998; Wesolowski et al., 2000; Boily et al., 2001; Gaboriaud and Ehrhardt, 2003). This idea has been an important part of the pathway connecting the molecular scale to thermodynamic models.

Real surfaces are, of course, never ideal, and recent studies have emphasized the relationship between structural and energetic heterogeneity in complex environments (Rudzinski et al., 2001; Boily et al., 2001). On sufficiently small scales, surface-surface interactions may alter the patterns of reactivity expected for idealized interfaces. In this paper, molecular dynamics simulations are used to compute proton distributions on faceted goethite particles 3 to 8 nm in size. The major finding is that, at these length scales, the simulated proton distributions do not at all reflect the sum of contributions from individual crystal faces. Instead, protons accumulate preferentially at edge regions defined by the acute intersections of (110)-(110) surfaces. Although there are several possible explanations for this behavior, we ascribe the effect to the more effective solvation of excess charge at the acute edges. This pattern of charge development is proposed to influence the thermodynamics and kinetics of acid-base, surface complexation and oxidation-reduction reactions in these systems.

2. BACKGROUND AND METHODS

Goethite (α-FeOOH) has received widespread attention in titration/sorption studies on low-temperature earth materials. Goethite is common in natural environments and is morphologically well characterized relative to other iron oxides and oxyhydroxides (Schwertmann and Cornell, 1991). Goethite crystals are often acicular and elongated on the crystallographic **c** direction. When they occur as euhedral crystals, they are commonly terminated on (110) on the elongated faces and are capped by (021) surfaces, as shown in Figure 1 (Weidler et al., 1998a). Faces are indexed in the Pbnm setting of space group #62 used in Schwertmann and Cornell (1991) with a = 0.4608 nm, b = 0.9956 nm, and c = 0.30215 nm. This is a different setting with the original structure determination of Szytula et al. (1968) (Pnma) but corresponds to the convention used for isostructural diaspore (AlOOH), and is in

* Author to whom correspondence should be addressed (jrrustad@ucdavis.edu).

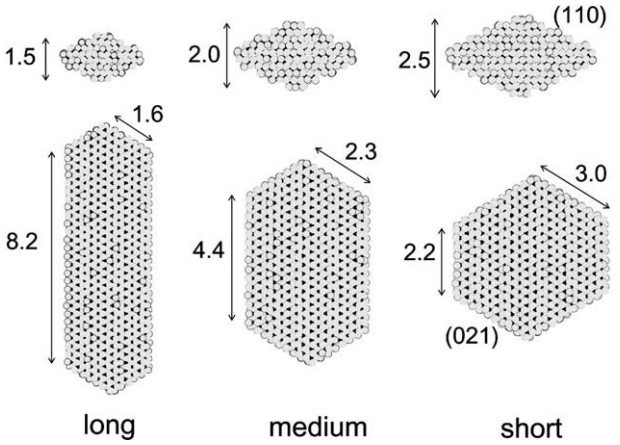

Fig. 1. Long, medium, and short goethite nanoparticles used in this study. Iron atoms are small dark atoms, oxygen atoms are large light atoms. Initial proton distributions are not shown. Numbers indicate dimensions of particle faces in nm. The particles were constructed to have nearly the same number of singly coordinated = FeO surface functional groups. Planes normal to the page are given in italics. The number of singly coordinated FeO surface functional groups, the Connolly solvent accessible surface area (nm^2), and the Connolly solvent-excluded volume (nm^3) (probe radius 0.14 nm) are as follows, Long (296, 125.2, 43.2); Medium (288, 108.5, 43.9); Short (298, 108.6, 46.6).

common use. Canonical surface structures differ significantly on the two faces, with the (021) surface presenting a higher density of singly coordinated = FeOH surface functional groups (3.4 FeOH sites/nm^2), while the (110) surface has 2.8 =FeOH sites/nm^2 when protonated to neutral charge (Rustad et al., 1996).

Goethite crystals exhibit varying degrees of acicularity, depending on the conditions of formation (Schwertmann and Cornell, 1991). Using the common morphology as a guide, idealized particles of goethite were extracted from the bulk solid, systematically varying the aspect ratio from high to low. The three particles denoted hereafter as long, medium, and short are shown in Figure 1, along with surface areas and volumes estimated using the method of Connolly (1985). In the bulk, goethite has two unique oxygen atoms, O1 and O2, each with three bonds to Fe^{3+}. The O1 oxide ions are also bound to a proton. After cutting the crystal out of the bulk, terminating on oxygen atoms, singly and doubly coordinated sites are left on the surface in addition to the two types of triply coordinated sites. The particles were brought to zero charge by adding protons to all the singly coordinated FeO sites (making ηOH groups) and doubly coordinated Fe_2O sites (making μOH groups). Triply coordinated O1 sites retain the protons they have in the bulk (they remain μ_3OH groups). Additional protons were added to randomly chosen FeOH sites (making ηH_2O groups) until the total charge ($3N_{Fe} - 2N_O + N_H$) was zero. In other words, every singly coordinated oxygen (FeO) has at least one proton (ηOH), and possibly two (ηOH_2). No protons were added to the triply coordinated O2 sites (which do not have protons in the bulk), and these μ_3O groups show no tendency to protonate during the simulation (which they are free to do). We did not investigate starting configurations having protonated O2 sites. The crystals were maintained in an idealized state by coupling each iron atom to its optimized site location using a weak harmonic spring. The particles are quite stable as constructed, and show no tendency to reconstruct upon removal from the bulk environment. The harmonic springs are introduced to inhibit rare surface hydration reactions from altering the surface structure. The reactions are very similar to those seen on Al_{13}^{7+} polynuclear ions, where they govern the lifetime of OH ions within the Al_{13} structure (Rustad et al., 2004a). While such surface hydration could certainly be relevant to the actual surface structure, such complications are ignored for the present; the hydrated groups are formed and destroyed on timescales too slow to average over in this study. Each particle was immersed in a bath of ~25,000 polarizable, heterolytically dissociable water molecules (described below), and molecular dynamics calculations were carried out over 2×10^5 timesteps (1 timestep = 0.27 fs). An extended Lagrangian method was used to treat oxide polarization as described in Rustad et al. (2004b). The temperature of the nuclear centers was 400 K and the fictitious dipole temperature was 5 K.

The slab systems shown in Figure 2 are ~5 nm on a side, ~2 nm thick, and are solvated by a layer of water ~3 nm thick. Molecular dynamics simulations for the slab systems were carried out for $\sim 10^6$ timesteps.

The interaction potentials have been described previously (Rustad, 2001 and references therein; Rustad et al., 2004a). The water potential is that of Halley et al. (1993), which is a polarizable, dissociating water model based on the work of Stillinger and David (1980). The short-range interactions for the Fe-water potential were fitted to first-principles electronic structure calculations (Curtiss et al., 1987). This Fe^{3+}-O^{2-}-H^+ has since proved surprisingly versatile and has been successfully applied to a wide range of problems in mineralogy, high-vacuum surface science, and interfacial chemistry (Rustad, 2001 and references therein; Rustad et al., 2004a; Rustad et al., 2004b). It has been demonstrated that the interaction potentials provide a reasonably accurate representation of acid/base reactions in the Fe^{3+}-O^{2-}-H^+ system of interest here.

The code used to do the simulations is available on request from the corresponding author, and also through the links at www.geology.ucdavis.edu/~Rustad. Briefly, the functional form consists of short-range O-O, O-H, and Fe-O interactions; monopole-monopole, monopole-dipole, and dipole-dipole interactions between pairs of oxygens; monopole-monopole and dipole-monopole interactions between O and H, and between O and Fe; and monopole-monopole interactions between H-H, H-Fe, and Fe-Fe. The dipole-monopole interactions between O-H and O-Fe are smoothly cut off as the O-H and Fe-O interionic distances r_{OH} and r_{FeO} approach zero.

Long-range interactions were treated using Wolf's method (Wolf et al., 1999). Comparisons between Wolf's method and the Ewald method on smaller slab systems showed that Wolf's method reproduced the surface functional group populations obtained using Ewald summation to within 1% for a cutoff distance of 1 nm. For cutoff distances less than 1 nm, agreement between Wolf's method and the Ewald method was rapidly degraded.

3. RESULTS AND DISCUSSION

After immersion in the water bath, both the particle and slab systems accumulate protons on the FeOH sites through the reaction $= FeOH + H_2O \rightarrow = FeOH_2^+ + OH^-$. This reaction was previously observed in simulations of magnetite-water interfaces (Rustad et al., 2003); however, the surface protonation is less complete in goethite than in magnetite because the $Fe^{2.5+}OH$ sites that are predominant on the magnetite surface are more basic than the $Fe^{3+}OH$ sites on goethite. The bridging μOH and μ_3OH sites are inert on simulation timescales.

It is impossible at this point to make any precise statement of the effective pH of the solution, as the accessible timescales do not permit convergence of pH calculations. Previous work on isolated Fe^{3+} in solution indicates an effective pH of ~4.6 for our Fe^{3+} - H_2O model (Rustad et al., 2004b), and this may be part of the reason why large numbers of protons are accumulating at the surface. However, the rather pedantic definition of charge accumulation, in this case simply counting up all protons attached to oxygens bound to irons, may be overly simplistic. It is possible that the association of protons with the oxide is much more subtle than direct attachment. For the present, it is assumed that the higher the number of ηH_2O groups on the surface, the more basic it is.

In the slab systems the charge accumulation per unit area on the (021) surface exceeds that of the (110) surface by 15%, as shown in Figure 3. In contrast, for the particle systems shown

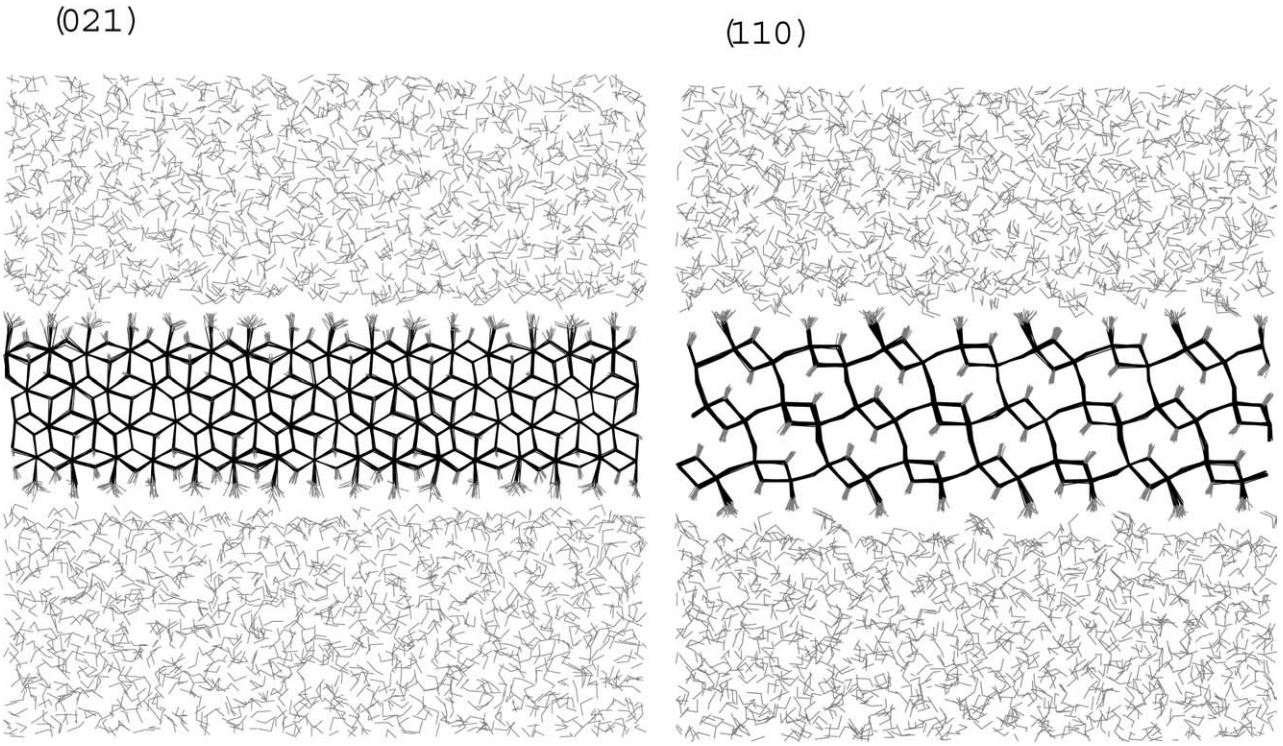

Fig. 2. Stick representation of atoms in the (021) (left), and (110) (right) slab systems. Fe-O bonds are dark, O-H bonds are gray. Systems are ~5 nm on a side.

in Figure 4, the long particle with the highest (110)/(021) ratio accumulates the most proton charge and the short particle with the lowest (110)/(021) ratio accumulates the least proton charge. Thus, at the length scales characteristic of the model systems, the proton distribution on the particles could not have been predicted from knowledge of the proton distributions on the individual faces.

The origin of the discrepancy between the infinite slab and particle systems can be seen in Figure 5, which shows the arrangements of the singly coordinated =FeO functional groups. The location of the spheres represents the average positions of oxygen atoms in the =FeO groups. The spheres are shaded according to their average protonation state over 10^5 timesteps. The figure reveals that the enhanced charge accumulation on the acicular particle is due to the high basicity of the FeO functional groups in the vicinity of the edges formed by the intersection of the (110) surfaces. Thus, while the interior regions of the (110) surface have a higher fraction of unprotonated sites, the high degree of protonation of the high-angle (110)-(110) edge regions dominates the distribution, giving the acicular crystal a higher basicity overall relative to the short crystal.

Different types of edges vary significantly in their Broensted acidity. In contrast to the positive charge accumulated at high-angle (110)-(110) edges, the low-angle (110)-(110) intersections and the (110)-(021) intersections appear to have little effect on protonation. The (021)-(021) intersections appear to have enhanced acidity. The behavior of the edges appears to depend rather specifically on the crystallographic relationships of the interacting surfaces.

Average Fe-O bond lengths on ηH_2O groups are significantly higher at the acute edge regions than at other sites. In Table 1, we give bond lengths and hydration numbers for the ηH_2O sites in regions 1, 2, 3, and 4 for the long particle as indicated in Figures 5a and 6b. Note that these averages are taken *only* for water molecules; if the site is deprotonated to OH^-, the site is not included in the average. The hydration number of a bound water molecule is defined by the number of

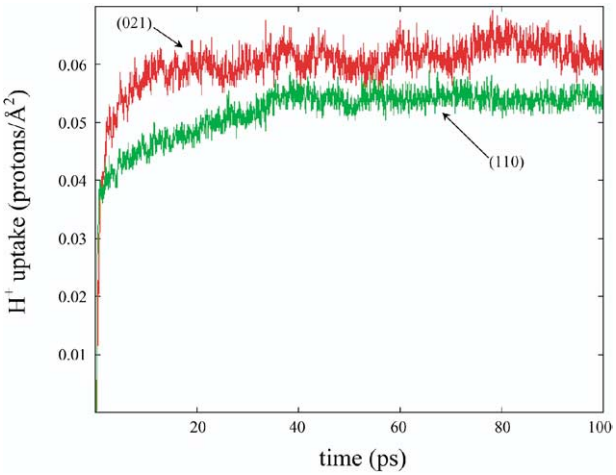

Fig. 3. Excess proton uptake on (110) and (021) slabs, in units of protons/Å^2, as a function of time over the first 100 picoseconds of the simulation. In the slab systems, each slab is initialized to neutral charge.

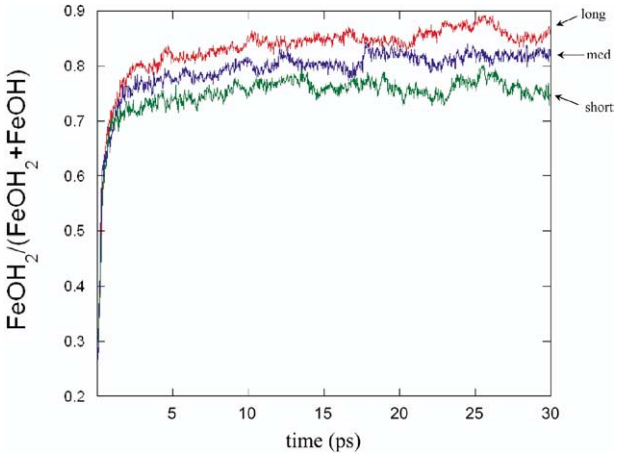

Fig. 4. Charge development on the long, medium, and short particles as a function of time over the first 30 picoseconds of the simulation. Graph gives the fraction of doubly protonated, singly coordinated sites (bound water molecules) divided by the total number of singly coordinated sites. Initial fractions are 0.28 for the long particles, 0.29 for the intermediate particles, and 0.32 for the short particles.

oxygen ions (not bound to an iron ion) within 3.2 Å of the molecule.

There are two underlying physicochemical causes that likely give rise to the observed charge distributions. First, it seems reasonable that the charge accumulations should take place in regions where the dielectric relaxation is large. The high-angle (110)-(110) intersections are surrounded to a greater extent by water, so it is perhaps not surprising that protons are preferentially accumulated in these regions (see Fig. 6a). A related effect is that, since the system overall is neutral, each positively charged surface functional group is associated with a hydroxide ion in solution. Thus, it is not only the ability of the water to solvate the positively charged surface functional group, but also the ability of the water to solvate the associated OH^- counterion that determines the surface charge distribution. Second, the singly coordinated ηH_2O and ηOH groups at the high-angle (110)-(110) edges do not have hydrogen bond donating μ_3OH groups underlying them, making them more basic (see Fig. 6b). These causes will impact the pH dependence of the charge distributions in different ways. If the effect is primarily governed by the dielectric relaxation of the solvent around the surface functional group, the dielectric will tend to solvate negative surface charges as well as it solvates positive surface charges, and the point of zero charge will be more or less independent of particle shape. In other words, under basic conditions, the edge sites would be preferentially *deprotonated* relative to the surface sites. If, however, the effect is primarily due to the intrinsic basicity of the edge sites due to crystallographic considerations, then the pH of zero charge of the long particles will be higher than that of the short crystals. The surprising similarity of the protonation states of oxygen ions in rows 1 and 2 is notable, given their wide differences in average bond length. This may indicate that dielectric effects are more important than crystallographic effects in determining the protonation states. We note that the bulk dielectric constant of our water model is somewhat underestimated, ~60 (as estimated through applying the Born model to the heat of solution of a

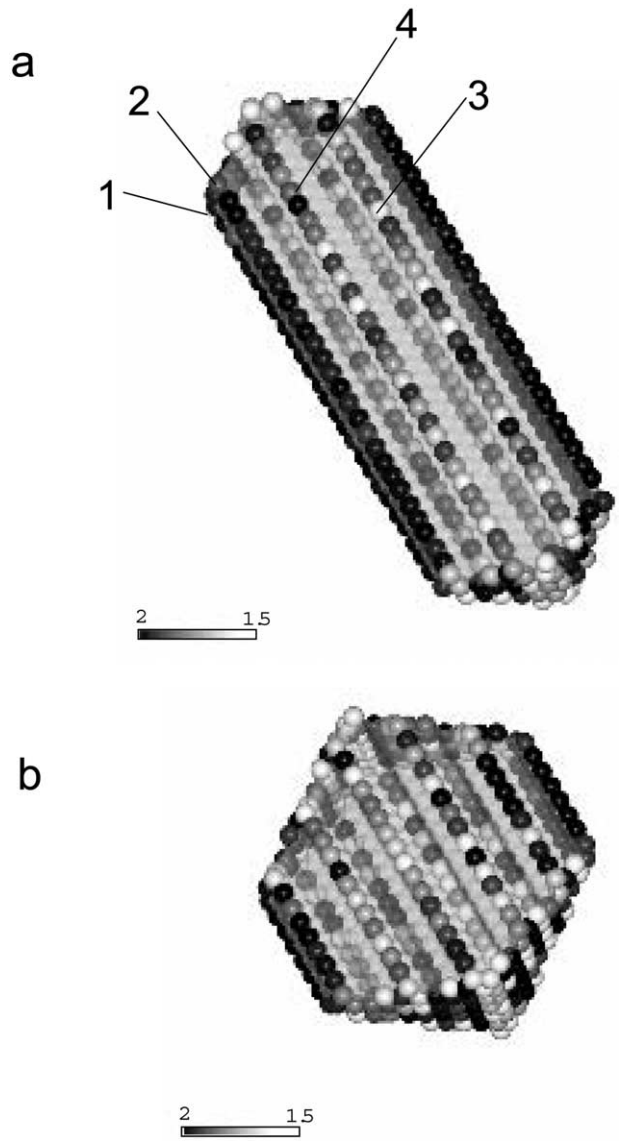

Fig. 5. Singly coordinated FeO functional groups indicated by spheres. The spheres are grayscale coded according to the average protonation states over the final 10^5 timesteps: (a) long particle and (b) short particle. In (a), oxygen rows 1, 2, 3, and 4 refer to the bond lengths and hydration numbers reported in Table 1. Groups 1 and 2 are near the high-angle (110)-(110) edges. The core of the particle, defined by the solvent accessible surface, is shown with translucent shading, i.e., oxygens on the underside of the particle are visible.

proton), so we are probably underestimating the dielectric response in the model calculations. It is also possible that the effective dielectric constant of water at an acute edge is different from that of water at a flat surface, but at present we ignore such effects.

Recent studies of proton uptake on goethite have noted that surface roughness appears to have a noticeable effect on the total proton uptake, but little effect on the pH of zero charge (Boily et al., 2001). Variations in the amount of proton uptake on a suite of goethite particles were interpreted as being the result of variability in surface roughness (Venema, 1997; Boily et al., 2001). The roughest surfaces were shown to have the

Table 1. Average Fe-O bond lengths for ηH_2O sites on rows indicated in Figure 5.

Row	Avg Fe-O bond length	Avg hyd. #	Avg. # of protons
1	2.21	1.5	1.98
2	2.11	1.3	1.95
3	2.14	0.9	1.73
4	2.12	0.9	1.71

largest proton uptake. The cause of this behavior was not well understood but was interpreted as a closer association of protons with the rough surfaces. The simulations on the model particles reported here may indicate that the higher uptake of the rough surfaces is due to dielectric effects favoring proton accumulation in edge regions. In the present study, such effects result solely from the dielectric response of water as there is no background electrolyte. In a system with background electrolyte, the electrolyte contribution to polarization around the surface charge would presumably also be enhanced in the edge region.

Inhomogeneous proton accumulation on colloidal particles and rough surfaces would have broad implications for ligand exchange and electron transfer reactions. Because sites at acute edges are more accessible to protons, and have longer Fe-O bonds to bound water sites, they should be preferentially reduced in oxidation-reduction reactions involving electron transfer from the solution phase to the solid phase. Similarly, electrons will be more mobile in edge regions for the same reason that decreasing pH increases Fe^{2+} -Fe^{3+} exchange rates in homogeneous solution. Ligand exchange kinetics would be similarly enhanced due to the swelling effects and increased M-O bond lengths at edge sites. The heterogeneity in the proton distributions will also influence the aggregation behavior of colloidal particles and provides a possible mechanism for electrostatic complementarity, allowing interparticle attachment pathways away from the point of zero charge (Penn and Banfield, 1998).

At some larger size, the behavior of the system overall must be predictable from the slabs. Currently, it is not computationally feasible to increase the simulated length scales by a factor of 10, as this would increase the computational effort by a factor of 1000, which is currently beyond our computer time limitations. While it would certainly be interesting to know where the crossover occurs, it is emphasized that the systems here are highly idealized. Weidler et al. (1998b) show, in a detailed study of the mesoscale crystallography of goethite, the presence of pores on the (110) faces bounded by (021) surfaces. Any real system will likely have significant roughness on 10 nm length scales, and hence, the edge effects highlighted in the simulations would still influence the charging behavior of the material. Thus, these results have some degree of generality and are not necessarily limited to the small length scales accessible through the simulations.

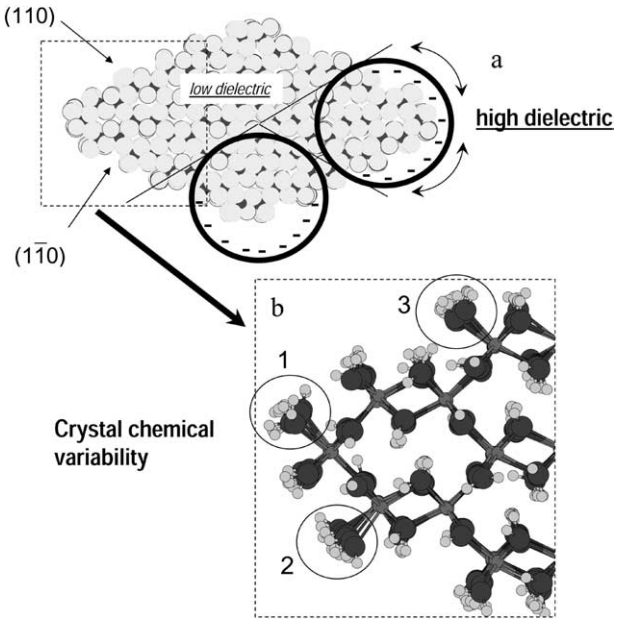

Fig. 6. Possible reasons for the inhomogeneous proton charge accumulation on the surfaces of the nanoparticles: (a) dielectric effects allowing more effective solvation of excess positive charge at acute edge sites; (b) crystal chemical variability in circled FeO sites due to finite size of particle; and (3) an Fe_3OH site underlies the circled FeO site. Such underlying sites are absent in (1) and (2), presumably increasing their proton affinities. Mechanism (a) should show up as an increase in proton uptake, but will have little effect on the zero point of charge; whereas mechanism (b) will shift the zero point of charge in the direction of increasing pH.

4. CONCLUSIONS

In a series of simple simulations, it has been shown, for idealized goethite particles of dimension $<$10 nm, that proton accumulation is significantly different than would have been predicted from the proton accumulations on slabs parallel to the faces defining the crystal morphology. These calculations underscore the potential complexities of surface charging on crystalline oxide materials at nanometer length scales and also reveal the inherent limitations of attempting to build any understanding of the chemical behavior of such systems in terms of a patchwork composite of interacting surfaces. These calculations suggest that a new direction is needed to build accurate structure-activity relationships for mineral-water interface geochemistry, one which must explicitly recognize the role of surface structural heterogeneity at length scales up to at least 10 nm. Progress in development of nanometer-scale structure-activity relationships will rely on the success of synthesizing oxide nanoparticles having known structures and well-characterized heterogeneity in this size range (Rowsell and Nazar, 2000; Allouche and Taulelle, 2003; Casey and Swaddle, 2003). Reactivity studies focused on these systems will be necessary, in addition to ongoing work focused on specific mineral surfaces, to put together interfacial models with any degree of molecular level truthfulness.

Acknowledgments—Dimitri Sverjensky, Lee Penn, Glenn Waychunas, Jill Banfield, and Bill Casey are thanked for interesting discussions associated with the manuscript. Comments from three anonymous reviewers greatly improved the paper. Support was generously provided by the Office of Basic Energy Sciences, Geosciences, and Chemical Sciences Research Programs of the US DOE. We thank the

Environmental Molecular Sciences Laboratory and the Molecular Sciences Computing Facility at the Pacific Northwest National Laboratory for a generous grant of computer time.

Associate editor: D. A. Sverjensky

REFERENCES

Allouche L. and Taulelle F. (2003) Conversion of Al-13 Keggin epsilon into Al-30: a reaction controlled by aluminum monomers. *Inorg. Chem. Comm.* **6,** 1167–1170.

Boily J. F., Lutzenkirchen J., Balmes O., Beattie J., and Sjoberg S. (2001) Modeling proton binding at the goethite (α-FeOOH)-water interface. *Colloids And Surfaces A-Physicochemical And Engineering Aspects* **179,** 11–27.

Brown G. E., Jr., Henrich V. E., Casey W. H., Clark D. L., Eggleston C., Felmy A., Goodman D. W., Gratzel M., Maciel G., McCarthy M. I., Nealson K. H., Sverjensky D. A., Toney M. F., and Zachara J. M. (1999) Metal oxide surfaces and their interactions with aqueous solutions and microbial organisms. *Chem. Rev.* **99,** 77–174.

Casey W. H. and Swaddle T. W. (2003) Why small? The use of small inorganic clusters to understand mineral surface and dissolution reactions in geochemistry. *Rev. Geophysics* **41,** 41–419.

Chambers S. A., Thevuthasan S., and Joyce S. A. (2000) Surface structure of MBE-grown Fe_3O_4(001) by X-ray photoelectron diffraction and scanning tunneling microscopy. *Surf. Sci.* **450,** L273–L279.

Connolly M. L. (1985) Computation of molecular volume. *J. Am. Chem. Soc.* **107,** 1118–1124.

Curtiss L. A., Halley J. W., Hautman J., and Rahman A. (1987) Nonadditivity of ab-initio pair potentials for molecular dynamics of multivalent transition metal ions in water. *J. Chem. Phys.* **86,** 2319–2327.

Felmy A. R. and Rustad J. R. (1998) Molecular statics calculations of proton binding to goethite surfaces: Thermodynamic modeling of the surface charging and protonation of goethite in aqueous solution. *Geochim. Cosmochim. Acta* **62,** 25–31.

Fenter P., Cheng L., Rihs S., Machesky M., Bedzyk M. J., and Sturchio N. C. (2000) Electrical double-layer structure at the rutile-water interface as observed in situ with small-period X-ray standing waves. *J. Colloid Interface Sci.* **225,** 154–165.

Gaboriaud F. and Ehrhardt J. (2003) Effects of different crystal faces on the surface charge of colloidal goethite (α-FeOOH) particles: An experimental and modeling study. *Geochim. Cosmochim. Acta* **67,** 967–983.

Halley J. W., Rustad J. R., and Rahman A. (1993) A polarizable, dissociating molecular dynamics model for liquid water. *J. Chem. Phys.* **98,** 4110–4119.

Hass K. C., Schneider W. F., Curioni A., and Andreoni W. (1998) The chemistry of water on alumina surfaces: Reaction dynamics from first principles. *Science* **282,** 265–268.

Henderson M. A., Joyce S. A., and Rustad J. R. (1998) Interaction of water with the (1 x 1) and (2 x 1) surfaces of α-Fe_2O_3(012). *Surf. Sci.* **417,** 66–81.

Hiemstra T. and VanRiemsdijk W. H. (1996) A surface structural approach to ion adsorption: The charge distribution (CD) model. *J. Colloid Interface Sci.* **179,** 488–508.

Hiemstra T., VanRiemsdijk W. H., and Bolt G. H. (1989) Multisite proton adsorption modeling at the solid-solution interface of (hydr)oxides - a new approach 1. Model description and evaluation of intrinsic reaction constants. *J. Colloid Interface Sci.* **133,** 91–104.

Kendelewicz T., Liu P., Doyle C. S., Brown G. E., Nelson E. J., and Chambers S. A (2000) Reaction of water with the (100) and (111) surfaces of Fe_3O_4. *Surf. Sci.* **453,** 32–46.

Koretsky C. M., Sverjensky D. A., and Sahai N. A. (1998) A model of surface site types on oxide and silicate minerals based on crystal chemistry: Implications for site types and densities, multi-site adsorption, surface infrared spectroscopy and dissolution kinetics. *Am. J. Sci.* **298,** 349–438.

Lodziana Z., Norskov J. K., and Stolze P. (2003) The stability of the hydroxylated (0001) surface of α-Al_2O_3. *J. Chem. Phys.* **118,** 11179–11188.

McCarthy M. I., Schenter G. K., Scamehorn C. A., Nicholas J. B. (1996) Structure and dynamics of the water/MgO interface. *J. Phys. Chem.* **100,** 16989–16995.

Morel F. M. M. and Hering J. G (1993) *Principles and Applications of Aquatic Chemistry*. John Wiley and Sons.

Parker S. C., de Leeuw N. H., and Redfern S. E. (1999) Atomistic simulation of oxide surfaces and their reactivity with water. *Faraday Discussions* **114,** 381–393.

Penn R. L. and Banfield J. F. (1998) Imperfect oriented attachment: Dislocation generation in defect-free nanocrystals. *Science* **281,** 969–971.

Rowsell J. and Nazar L. F. (2000) Speciation and thermal transformation in alumina sols: Structures of the polyhydroxyoxoaluminum cluster $[Al_{30}O_8(OH)_{56}(H_2O)_{26}]^{18+}$ and its δ-Keggin moiete. *J. Am. Chem. Soc.* **122,** 3777–3778.

Rudzinski W., Lee S. L., Yan C. C. S., and Panczyk T. (2001) A fractal approach to adsorption on heterogeneous solid surfaces. 1. The relationship between geometric and energetic surface heterogeneities. *J. Phys. Chem. B* **105,** 10847–10856.

Rustad J. R. (2001) Molecular models of surface relaxation, hydroxylation and surface charging at oxide-water interfaces. In *Molecular Modeling Theory: Applications in the Geosciences*, Reviews in Mineralogy & Geochemistry, Vol. 42 (ed. J. D. Kubicki and R. T. Cygan), pp 169–197. Mineralogical Society of America.

Rustad J. R., Felmy A. R., and Hay B. P. (1996) Molecular statics calculations of proton binding to goethite surfaces: A new approach to estimation of stability constants for multisite surface complexation models. *Geochim. Cosmochim. Acta* **60,** 1563–1576.

Rustad J. R., Wasserman E., and Felmy A. R. (1999) A molecular dynamics investigation of surface reconstruction on magnetite (001). *Surf. Sci.* **432,** L583–L588.

Rustad J. R., Felmy A. R., and Bylaska E. J. (2003) Molecular simulation of the magnetite-water interface. *Geochim. Cosmochim. Acta* **67,** 1001–1016.

Rustad J. R., Loring J. S., and Casey W. H. (2004a) Oxygen exchange pathways in aluminum polyoxocations. *Geochim. Cosmochim. Acta* **68,** 3011–3017.

Rustad J. R., Rosso K. M., and Felmy A. R. (2004b) A molecular dynamics investigation of ferrous-ferric electron transfer in a hydrolyzing aqueous solution: Calculation of the pH dependence of the diabatic transfer barrier and the potential of mean force. *J. Chem. Phys.* **120,** 7607–7615.

Schwertmann U. and Cornell R. M. (1991) *Iron Oxides in the Laboratory*. VCH Weinheim.

Shapovalov V., Wang Y., Truong T. N. (2003) Theoretical analysis of the electronic spectra of water adsorbed on the rutile TiO_2 (110) and MgO (100) surfaces. *Chem. Phys. Lett.* **375,** 321–327.

Sposito G. (2004) *Surface Chemistry of Natural Particles*. Oxford University Press.

Stillinger F. H. and David C. W. (1980) Study of the water octamer using the polarization model of molecular interactions. *J. Chem. Phys.* **73,** 3384–3389.

Stirniman M. J., Huang C., Smith R. S., Joyce S. A., and Kay B. D. (1996) The adsorption and desorption of water on single crystal MgO(100): The role of surface defects. *J. Chem. Phys.* **105,** 1295–1298.

Sverjensky D. A. and Sahai N. (1996) Theoretical prediction of single-site surface-protonation equilibrium constants for oxides and silicates in water. *Geochim. Cosmochim. Acta* **60,** 3773–3797.

Szytula A., Burewicz A., Dimitrijewic Z., Krasnicki S., Rzany H., Todorovic J., Wanic A., and Wolski W. (1968) Neutron diffraction studies of α-FeOOH. *Physica Status Solidii* **26,** 429–434.

Trainor T. P., Eng P. J., Brown G. E., Robinson I. K., De Santis M. (2002) Crystal truncation rod diffraction study of the alpha-Al_2O_3 (1(1)over-bar-0 2) surface. *Surf. Sci.* **496,** 238–250.

Venema P. (1997) *Charging and ion adsorption behavior of different iron (hydr)oxides* Ph.D. Thesis, University of Wageningen Agricultural University, The Netherlands.

Wang X. G., Weiss W., Shaikhutdinov S. K., Ritter M., Petersen M., Wagner F., Schlogl R., Scheffler M. (1998) The hematite (α-Fe_2O_3) (0001) surface: Evidence for domains of distinct chemistry. *Phys. Rev. Lett.* **81,** 1038–1041.

Wasserman E., Rustad J. R., Felmy A. R., Hay B. P., Halley J. W. (1997) Ewald methods for polarizable surfaces with application to hydroxylation and hydrogen bonding on the (012) and (001) surfaces of α-Fe_2O_3. *Surf. Sci.* **385,** 217–239.

Weidler P. G., Hug S. J., Wetche T. P., Hiemstra T. (1998a) Determination of growth rates of (100) and (110) faces of synthetic goethite by scanning force microscopy. *Geochim Cosmochim. Acta* **62,** 3407–3412.

Weidler P. G., Degovics G., and Laggner P. (1998b) Surface roughness created by acidic dissolution of synthetic goethite monitored with SAXS and N_2adsorption isotherms. *J. Colloid Interface Sci.* **197,** 1–8.

Wesolowski D. J., Machesky M. L., Palmer D. A., and Anovitz L. M. (2000) Magnetite surface charge studies to 290 degrees C from in situ pH titrations. *Chem. Geology* **167,** 193–229.

Wolf D., Keblinski P., Phillpot S. R., and Eggebrecht J. (1999) Exact method for the simulation of Coulombic systems by spherically truncated, pairwise r^{-1} summation. *J. Chem. Phys.* **110,** 8254–8282.

Zhang Z., Fenter P., Cheng L., Sturchio N. C., Bedzyk M. J., Predota M., Bandura A., Kubicki J. D., Lvov S. N., Cummings P. T., Chialvo A. A., Ridley M. K., Benezeth P., Anovitz L., Palmer D. A., Machesky M. L., and Wesolowski D. J. (2004) Ion adsorption at the rutile-water interface: Linking molecular and macroscopic properties. *Langmuir* **20,** 4954–4969.